BEHAVIOUR OF HYBRID FERRO FIBER CONCRETE (HFFC) UNDER AXIAL COMPRESSION

K.Ramesh* D.R.Seshu and M.Prabhakar*****

The combination of fiber reinforced concrete and ferrocement can be used in developing a concrete composite with large ductility, which is required in structures subjected to seismic forces. Such a concrete composite can be termed as HYBRID FERRO FIBER CONCRETE (HFFC). This paper presents an experimental investigation on the behavior of HFFC under axial compression. The parameters varied include (1) Specific surface factor (S_f) of ferrocement shell which influences the behavior of ferrocement, (2) Reinforcing index (RI) of steel fiber concrete which influences the behavior of FRC. One hundred and sixty eight prism specimens of size 150mm x 150mm x 300mm were tested under strain-controlled rate of loading. The results indicated that the combined use of ferrocement and fibers in Hybrid ferro fiber concrete has improved the ultimate strength; strain at ultimate strength and the ductility. The improvement is proportional to the specific surface factor (S_f) of ferrocement shell for a given confinement index (C_i) of lateral reinforcement and reinforcing index (RI) of steel fiber reinforced concrete.

NOTATION

b, d	=	Lateral dimensions of prism
f_y	=	Yield strength of longitudinal / tie / fiber / mesh wire (Table 1)
A_s	=	Area of longitudinal steel
f_c'	=	Strength of unconfined concrete(Plain concrete prism strength)
ε_c'	=	Strain at peak of unconfined concrete (Plain concrete prism)
f_u'	=	Strength of tie confined fiber reinforced concrete (CFRC)
	=	$f_c'(1 + 0.55C_i)(1.0228 + 0.1024(RI))$ [13,14]
ε_u	=	Strain at ultimate of Tie confined fiber reinforced concrete [13,14]
A_g	=	Gross cross sectional area
C_i	=	Confinement index [10] $= (P_b - P_{bb})(f_v / f_c')\sqrt{(b/s)}$
P_b	=	Ratio of volume of transverse steel to the volume of concrete
P_{bb}	=	Ratio of volume of transverse steel to the volume of concrete Corresponding to a limiting pitch equal to 1.5 b
f_v	=	Stress in lateral ties
s	=	Spacing of lateral ties
ε_{fu}	=	Strain at peak of HFFC
$\varepsilon_{0.85\,fu}$	=	strain at 85% of peak of HFFC in the descending portion of stress strain curve

* Research scholar, Dept. Civil Engineering, Regional Engineering College, Warangal - 506 004 and Lecturer at KITS, WARANGAL - 506 015, Andhra Pradesh, INDIA. E-mail:<kramesh02@rediff mail.com>
** Assistant Professor, Dept. of Civil Eng. R.E.C, Warangal - 506 004, E-mail:<drseshu@recw.ernet.in>
*** Professor of civil Eng. and Principal, KITS, Warangal - 506 015.

$\varepsilon_{0.85\,u}$ = Strain at 85% of peak of CFRC in the descending portion of stress strain curve
K_f = Load ratio explained in the paper
f'_u = Peak strength of HFFC
RI = Reinforcing Index (Product of weight fraction of fiber (W_f) and aspect ratio of fiber)
W_f = Ratio of weight of steel fiber and weight of concrete
S_f = Specific surface factor

INTRODUCTION

Seismic resistant design of structures demands high ductility. The ductility of concrete is being improved at present by confining it in steel binders, as ties in compression members and as stirrups in beams. It has been reported [3] that a concrete strain of 0.01 is sufficient to give full redistribution of moments, which results in the use of procedures of plastic analysis for analysis of concrete structures also. However, it can be seen that the higher the degree of indeterminacy of the structures the more will be the concrete strain at failure and consequently the rotation capacity required at the first plastic hinge which will form in the structure. The critical section in statically indeterminate structures at which first hinge forms are incidentally also the sections having maximum shear force. The stirrup reinforcement, which is provided, has to take care of shear at that section and simultaneously provide confinement. It has been established by previous researcher [12] that only the stirrup reinforcement provided beyond what is required for resisting shear failure will only provide confinement. Hence with practical minimum spacing that can be provided at the critical sections, there is limitation to the quantity of confinement, which can be provided by the stirrups. Moreover, confinement of a column using a sophisticated arrangement of closely spaced stirrups not only interrupts the continuity and creates plane of weakness between the core and the concrete cover, but it also adds to the problem of congestion. Thus, it may not be possible to sufficiently confine the structure by providing the laterals alone. Hence, it would be useful if a supplementary confinement in addition to the laterals can be provided at the critical sections or a better alternative to confinement can be devised. Recently the combination of steel fiber and reinforced concrete (CFRC) [5,13,14] was made use in improving ductility. Such concrete was termed as Confined Fiber Reinforced Concrete (CFRC). There is limitation to the quantity of passive confinement offered by steel fiber due to balling of fiber at higher dosages. Ferrocement shell (casing) can be used to CFRC for the further improvement in degree of confinement. Such concrete, which is a combination of ferrocement, fiber reinforced concrete and lateral reinforcement can be termed as HYBRID FERRO FIBER CONCRETE (HFFC). The Present investigation is an attempt to study the confining effect of the ferrocement shell, provided in addition to rectangular ties on fiber reinforced concrete under axial compression.

EXPERIMENTAL STUDY

Scheme of experimental work

The experimental program was designed to study the behavior of fiber rein forced concrete confined by ferrocement shell (HFFC) under axial compression by testing prisms of size 150mm x 150mm x 300mm. The variables in the study are specific surface factor (S_f), which controls the behavior of ferrocement, reinforcing index (RI) of steel fiber, which controls the behavior of core fiber reinforced concrete. A constant lateral tie spacing adopted in this investigation was 60 mm; the confinement index (C_i) takes into account the effect of lateral tie confinement. Specific surface factor is the product

of specific surface ratio and yield stress of mesh wires in the direction of force divided by the strength of plain mortar [11]. Specific surface ratio is the ratio of the total surface area of contact of reinforcement wires present per unit length of the specimen in the direction of the application of the load in a given width and thickness of ferrocement shell to the volume of mortar. The reinforcing index (RI) of the steel fiber is the product of weight fraction (W_f) of steel fiber and the aspect ratio of the fiber. The weight fraction (w_f) is the ratio of weight of steel fiber and weight of concrete.

The program consisted of casting and testing of 168 prisms, which were cast in 10 batches (Viz., A, B, C, D, E, F, G, H and I – series). The prisms in each batch (i.e. A- series to F- series) are divided into six sets. The prisms in each batch (i.e. G-series to I- series) are divided into five sets. In both the cases, first set consist of plain concrete prisms and in the second set, fiber reinforced concrete prisms without any ferrocement shell as additional confinement were cast. In the remaining sets, fiber reinforced concrete prisms with ferrocement shell as additional confinement (HFFC Prisms) were cast. Except in first set, the amount of reinforcement (Longitudinal and lateral steel) was maintained constant and equal to that provided in the prisms of second set. But the amount of ferrocement shell confinement varied by varying the specific surface factor (S_f). Since the effect of confinement on fiber reinforced concrete due to lateral reinforcement [13,14] was already known, the effect of confinement due to ferrocement shell can be separated. The details of prisms tested are given in Table. 1.

Materials Used

The galvanized woven wire mesh of square grid fabric was used in ferrocement. The ties and longitudinal steel used in the prisms were made of mild steel and galvanized iron steel respectively. The cement used was OPC of 43 grade conforming to IS: 8112 – 1981. Machine crushed hard granite chips passing through 12.5 mm IS sieve and retained on 4.75 mm IS sieve was used as coarse aggregate throughout the work. River sand procured locally was used for fine aggregate. Fine aggregate passing through 2.36mm IS sieve was used in core fiber reinforced concrete and passing through 1.18 mm IS Sieve was used in ferrocement shell. Core fiber reinforced concrete and in ferrocement shell respectively. The same concrete (1:1.8:2.5 and W/C = 0.5) was used in the entire study. The mortar used for the ferrocement shell has the mix proportion of one part cement and two parts sand (i.e., 1:2) with a water cement ratio of 0.6.

Preparation of specimen

After the fabrication of ferrocement cages using ties and longitudinal steel, a sufficient number of wire mesh layers to provide the required S_f were wrapped over the ties tightly by giving an overlap of 50 mm. The mesh was stitched thrice so as not to fail by splitting of the mesh. Fig. 1(a) shows the reinforcement details of specimen. Fig. 1(b) shows the mould used for casting the prisms.

Table 1 Detail of Prisms Tested

S.No	Specimen Designation	Lateral Reinforcement			Longitudinal reinforcement		Mesh Reinforcement					Steel Fiber		f_c' (Mpa)	ε_c' 10^{-5}
		Dia. (mm)	f_y (Mpa)	C_i	Dia. (mm)	f_y (Mpa)	Dia. (mm)	f_y (Mpa)	Spacing (mm)	No.of Layers	S_f	V_f %	RI		
1	A0	6.42	300	0.35	4.00	390	0.33	370	1.78	0	0	0	0	23.06	160
2	A1	6.42	300	0.35	4.00	390	0.33	370	1.78	1	4.5	0	0	23.06	160
3	A2	6.42	300	0.35	4.00	390	0.33	370	1.78	2	9.0	0	0	23.06	160
4	A3	6.42	300	0.35	4.00	390	0.33	370	1.78	3	13.5	0	0	23.06	160
5	A4	6.42	300	0.35	4.00	390	0.33	370	1.78	4	18.0	0	0	23.06	160
6	B0	6.42	300	0.39	4.00	390	0.33	370	1.78	0	0	0.6	1.48	20.1	165
7	B1	6.42	300	0.39	4.00	390	0.33	370	1.78	1	4.5	0.6	1.48	20.1	165
8	B2	6.42	300	0.39	4.00	390	0.33	370	1.78	2	9.0	0.6	1.48	20.1	165
9	B3	6.42	300	0.39	4.00	390	0.33	370	1.78	3	13.5	0.6	1.48	20.1	165
10	B4	6.42	300	0.39	4.00	390	0.33	370	1.78	4	18.0	0.6	1.48	20.1	165
11	C0	6.42	300	0.37	4.00	390	0.33	370	1.78	0	0	1.2	2.96	21.74	162
12	C1	6.42	300	0.37	4.00	390	0.33	370	1.78	1	4.5	1.2	2.96	21.74	162
13	C2	6.42	300	0.37	4.00	390	0.33	370	1.78	2	9.0	1.2	2.96	21.74	162
14	C3	6.42	300	0.37	4.00	390	0.33	370	1.78	3	13.5	1.2	2.96	21.74	162
15	C4	6.42	300	0.37	4.00	390	0.33	370	1.78	4	18.0	1.2	2.96	21.74	162
16	D0	7.00	385	0.41	4.00	390	0.27	275	2.06	0	0	0	0	23.54	180
17	D1	7.00	385	0.41	4.00	390	0.27	275	2.06	1	3.2	0	0	23.54	180
18	D2	7.00	385	0.41	4.00	390	0.27	275	2.06	2	6.4	0	0	23.54	180
19	D3	7.00	385	0.41	4.00	390	0.27	275	2.06	3	9.6	0	0	23.54	180
20	D4	7.00	385	0.41	4.00	390	0.27	275	2.06	4	12.8	0	0	23.54	180
21	E0	7.00	385	0.40	4.00	390	0.27	275	2.06	0	0	0.3	0.74	22.90	200
22	E1	7.00	385	0.40	4.00	390	0.27	275	2.06	1	3.2	0.3	0.74	22.90	200

Table 1 Detail of Prisms Tested (cont.)

S.No	Specimen Designation	Lateral Reinforcement			Longitudinal reinforcement		Mesh Reinforcement					Steel Fiber		f_c' (Mpa)	ε_c' 10^{-5}
		Dia. (mm)	f_y (Mpa)	C_t	Dia. (mm)	f_y (Mpa)	Dia. (mm)	f_y (Mpa)	Spacing (mm)	No.of Layers	S_f	V_f %	RI		
23	E2	7.00	385	0.40	4.00	390	0.27	275	2.06	2	6.4	0.3	0.74	22.90	200
24	E3	7.00	385	0.40	4.00	390	0.27	275	2.06	3	9.6	0.3	0.74	22.90	200
25	E4	7.00	385	0.40	4.00	390	0.27	275	2.06	4	12.8	0.3	0.74	22.90	200
26	F0	7.00	385	0.40	4.00	390	0.27	275	2.06	0	0	0.9	2.21	23.00	195
27	F1	7.00	385	0.40	4.00	390	0.27	275	2.06	1	3.2	0.9	2.21	23.00	195
28	F2	7.00	385	0.40	4.00	390	0.27	275	2.06	2	6.4	0.9	2.21	23.00	195
29	F3	7.00	385	0.40	4.00	390	0.27	275	2.06	3	9.6	0.9	2.21	23.00	195
30	F4	7.00	385	0.40	4.00	390	0.27	275	2.06	4	12.8	0.9	2.21	23.00	195
31	G0	7.00	448	0.37	3.00	350	0.27	250	3.1	0	0	0	0	26.25	190
32	G2	7.00	448	0.37	3.00	350	0.27	250	3.1	2	3.79	0	0	26.25	190
33	G3	7.00	448	0.37	3.00	350	0.27	250	3.1	3	5.68	0	0	26.25	190
34	G4	7.00	448	0.37	3.00	350	0.27	250	3.1	4	7.58	0	0	26.25	190
35	H0	7.00	448	0.37	3.00	350	0.27	250	3.1	0	0	0.4	0.983	26.25	210
36	H2	7.00	448	0.37	3.00	350	0.27	250	3.1	2	3.79	0.4	0.983	26.25	210
37	H3	7.00	448	0.37	3.00	350	0.27	250	3.1	3	5.68	0.4	0.983	26.25	210
38	H4	7.00	448	0.37	3.00	350	0.27	250	3.1	4	7.58	0.4	0.983	26.25	210
39	I0	7.00	448	0.37	3.00	350	0.27	250	3.1	0	0	0.8	1.965	26.25	205
40	I2	7.00	448	0.37	3.00	350	0.27	250	3.1	2	3.79	0.8	1.965	26.25	205
41	I3	7.00	448	0.37	3.00	350	0.27	250	3.1	3	5.68	0.8	1.965	26.25	205
42	I4	7.00	448	0.37	3.00	350	0.27	250	3.1	4	7.58	0.8	1.965	26.25	205
43	J0	7.00	448	0.40	3.00	350	0.27	250	3.1	0	0	1.2	2.96	24.25	210
44	J2	7.00	448	0.40	3.00	350	0.27	250	3.1	2	3.79	1.2	2.96	24.25	210
45	J3	7.00	448	0.40	3.00	350	0.27	250	3.1	3	5.68	1.2	2.96	24.25	210
46	J4	7.00	448	0.40	3.00	350	0.27	250	3.1	4	7.58	1.2	2.96	24.25	210

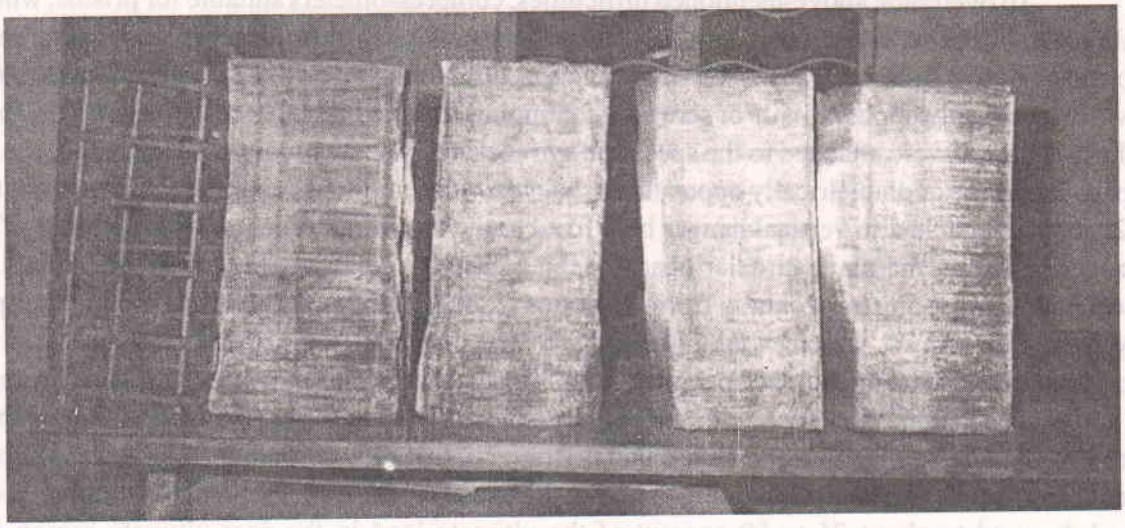

Fig. 1. (a) Reinforcement details of the specimens

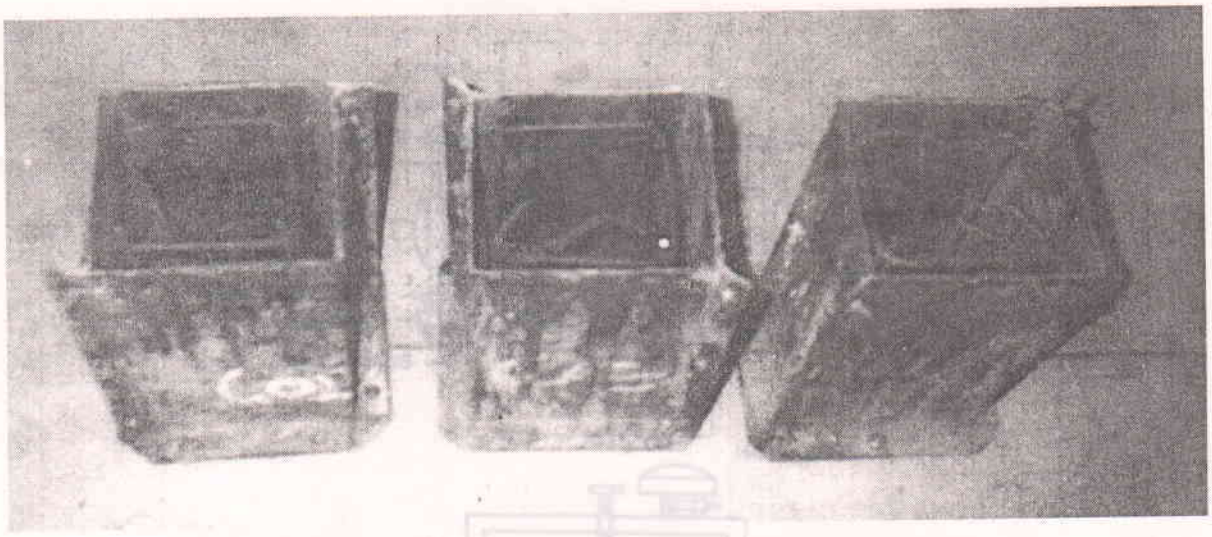

Fig. 1. (b) Moulds used for casting the prisms

Casting of the specimen

The prepared cage of reinforcement was kept in moulds carefully. Spacer rods of 3mm diameter galvanized iron wires were kept temporarily in between the layers of mesh to maintain spacing between the layers. The prisms were cast in the vertical position. First, the gap between the mould and the reinforcement was filled to about half the height of the mould using cement mortar, and then fiber reinforced concrete was placed inside the mesh up to the same level. Then, a needle vibrator was used to compact the core fiber reinforced concrete. The mould was filled in three layers using the same technique. The top face of the prism specimen was capped with a rich cement paste. The specimen was demoulded 48 hours after casting and cured for 28 days in a curing pond.

Testing

The cured specimens were capped with plaster of Paris before testing, to provide a smooth loading surface. A Tinius – Olsen testing machine of 1810 KN capacity was used for testing the prisms

under axial compression. From the studies of previous investigators [12] who worked on concrete confined with ties, it was observed that the cover concrete spalled off at about 90 percent of the ultimate load, the resistance strain gauges and Demec points fixed to the concrete surface usually came off along the concrete. In addition, the compressometer designed to measure the strains in standard concrete cylinders could not be fitted to the square prisms.

To overcome above-mentioned difficulties, compressometers suitable for prisms, which were fabricated by the earlier investigators [12] on confined concrete, were adopted. Each compressometer consisted of two square frames; a top frame and a bottom frame made of 12mm square mild steel bars. Two diametrically opposite pairs of screws at four points attached each frame to the concrete specimen. The two frames were attached to the specimen symmetrically at the required gauge length, i.e.150mm apart. Two pairs of diametrically opposite dial gauges with a minimum count of 0.002mm and travel of 12mm were attached to vertical hanger bars fixed to the top frame. The movable spindles of the dial gauges rested on the plane circular heads of the adjustable screws, which were positioned in mild steel plates projecting horizontally from the bottom frame. The frames were attached to the specimen by means of screws, which would fit snugly to the concrete. Fig. 2(a) shows the details of the compressometer attached to the specimen. Fig. 2(b) shows the photograph of the same arrangement.

The capped specimen with the compressometer attached was placed on the movable cross head of the testing machine and tested under strain control rate of loading. The deformations were noted and strains were calculated. Fig. 3 shows the test arrangement. The test was continued until the load dropped to about 75 to 80 percent of the ultimate load in the post ultimate region for both confined and unconfined prism specimens.

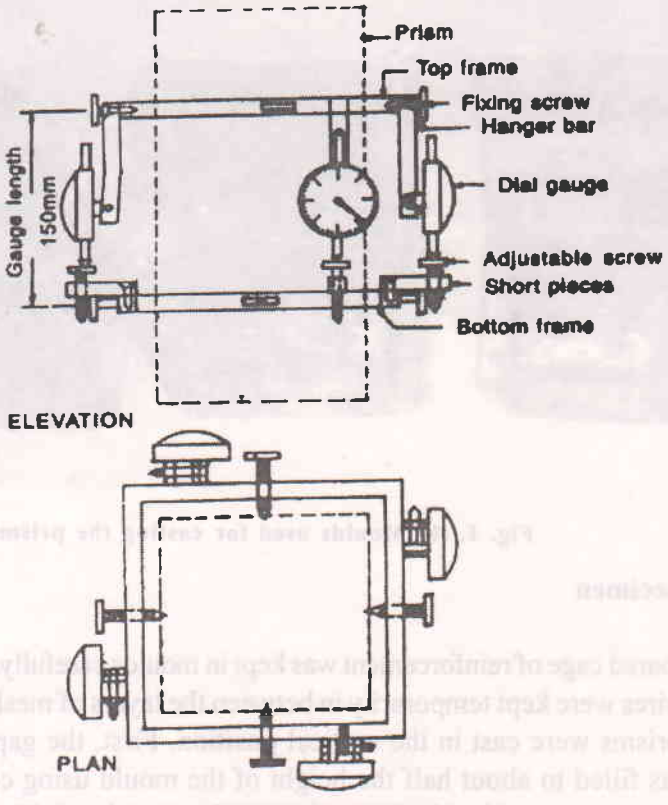

Fig. 2. (a) Detail of compressometer

Fig. 2. (b) Compressometer attached to the prism

INTERPRETATION AND DISCUSSION OF TEST RESULTS

Behavior of test specimens under load

(A) General: The load increased rapidly in the initial stages up to about 75 percent of the peak load and thereafter increased at a slower rate until the peak load was reached, Tests were continued until the peak load dropped to about 0.75 to 0.80 times the peak load. Beyond the peak load, the strains increased at a rapid rate and were accompanied by a decrease in the load carrying capacity of the specimen.

(B) Reinforced Concrete (RC) Specimens: In the case of RC specimens, vertical cracks appeared in the cover region at about half of the peak load. As load increased, the number of cracks increased and the width of cracks widened. The spalling of concrete cover was noticed before the peak load (i.e. at about 90 percent of peak load) was reached, but it was severe after passing the peak load.

(C) Confined Fiber Reinforced Concrete (CFRC) Specimens: In the case of CFRC specimens, fine vertical cracks appeared on the surface of the specimen at about 80 percent of the peak load. With the increase of load, the number of cracks increased at a reduced rate compared to RC specimens. The behavior of all CFRC specimens up to 75 percent of the peak load of the confined RC specimens was about the same. Beyond the peak load, the fine vertical cracks widened. The extent of the cracking and rate of decrease in load after the peak (in descending portion of stress – strain curve) depends up on the reinforcing index (RI) of steel fiber; if the confinement indicated by C_i of lateral reinforcement is the

same. The higher the RI, the lower is the rate of decrease in load and the extent of sapling. This may be due to the internal crack arresting mechanism, dimensional stability as well as integrity of the material caused by the large volume fraction of steel fiber present in the concrete. The maximum stress and strain at peak load and the strain at 85 percent of peak load in the descending portion of the stress-strain curve increased as RI increased with the same C_i.

(D) Hybrid Ferro Fiber Concrete (HFFC) Specimens: In the case of HFFC specimens, fine vertical cracks at about 85 percent of the peak load. With the increase in load, the number of cracks increased and the width of cracks increased at a reduced rate compared to that of RC specimens. The behavior of all the HFFC specimens up to 85 percent of the peak load of the confined RC specimens was about the same. Beyond the peak loads, the mesh wires started bulging and the mortar cover over the mesh wires started spalling. The extent of spalling became severe only after the load dropped to about 0.7 to 0.8 times the peak load. The extent of spalling and the rate of decrease of load after the peak (in descending branch of stress-strain curve) depended upon the specific surface factor (S_f) of the ferrocement shell if the tie confinement, as indicated by the confinement index (C_i) and the passive confinement of steel fiber indicated by the RI of FRC was the same. The higher the specific surface factor (S_f), the lower the rate of decrease of load and the extent of spalling. This may be due to the improvement of dimensional stability as well as the integrity of the material, caused by the presence of large specific surface factor of the ferrocement shell provided as additional confinement to the core fiber reinforced concrete. The highest strain observed at maximum stress of any specimen was 0.03, and that at 0.85 times the maximum stress was 0.07 on the descending branch of the stress-strain curve, compared to 0.002 and 0.0035 for plain concrete specimens respectively.

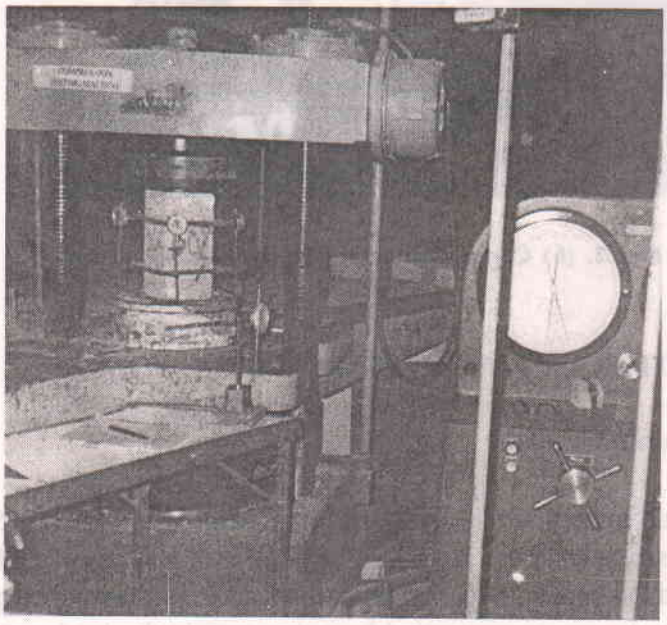

Fig. 3. Details of Specimen under test

Experimental stress-strain curves

From observed data, for a given specimen, the longitudinal deformations were calculated from the average readings of the four dial gauges of the compressometer. As there was no severe spalling in HFFC specimens until the load dropped by about 20 to 25 percent of peak load, the specimens were treated as dimensionally stable and hence the gross cross sectional area was used in calculating the stress values. Stress-strain curves were drawn for three companion specimens of a set with the same origin, and the average curve was taken to represent the set. Such average curves for all the sets of one typical batch with a common origin are shown in Fig. 4.

Effect of specific surface factor on:

(i) **Ultimate strength**: The ultimate strength of fiber reinforced concrete increased with the increase in S_f for the same level of tie confinement (C_i) and the reinforcing index RI of steel fiber. To quantify the effect of ferrocement shell confinement on ultimate strength, the effect of confinement due to combination of steel fiber and lateral reinforcement is separated using the following equation:

$$f_u A_g = K f_c' A_g \quad \text{...(1)}$$

= the load taken by the tie confined fiber reinforced concrete[14]

Where, $K = (1 + 0.55\, C_i)\,(1.0228 + 0.1024\, RI)$ ...(2)

$$C_i = (P_b - P_{bb})(f_v / f_c')\sqrt{(b/s)}$$

Since the ultimate load carrying capacity (P) is experimentally determined $(P - A_s f_y)$ gives the contribution to load carrying capacity due to ferrocement shell confinement. This value is non- dimensionalized by dividing with $f_u A_g$. This means that $K_f = (P - A_s f_y) / f_u A_g$ gives the strength of Hybrid ferro fiber concrete as the ratio of fiber reinforced concrete confined by lateral ties only. A plot of K_f versus RI is given in Fig. 5. An examination of plot shows that there is linear relationship between K_f and S_f. The linear equation thus obtained with 95 percent confidence limits is given below:

$$K_f = (0.99 \pm 0.0149) + (0.0166 \pm 0.0014) S_f \quad \text{...(3)}$$

$$K_f \approx (1.0 + 0.0166\, S_f) \quad \text{...(4)}$$

Hence the final equation for load carrying capacity (P) of Hybrid ferro fiber concrete prism is

$$P = f_c' (1 + 0.55 C_i)\,(1.0228 + 0.1024\, RI)\,(1.0 + 0.0166\, S_f)\, A_g + f_y A_s \quad \text{...(5)}$$

(ii) **Strain peak strength:** The ultimate strain increased with an increase in specific surface ...ctor (S_f). Fig. 6 shows plot between the ratio observed strain) (ε_{fu}) at the peak strength of HFFC to ...ical strain (ε_u) at the peak strength of tie confined fiber reinforced concrete and the specific ... An examination of plot clearly indicates that there is a linear relationship between ... ε_u).

th

A straight line fit between the ratio $(\varepsilon_{fu}/\varepsilon_u)$ and specific surface factor S_f resulted the following equation:

$$(\varepsilon_{fu}/\varepsilon_u) = (1.0 \pm 0.088) + (0.1359 \pm 0.0083)S_f \quad ...(6)$$

The strain at the peak strength of a HFFC prism can be rewritten in the following form:

$$\varepsilon_{fu} = \varepsilon_c'(1.0 + 5.2\ C_f)\ (0.9899 + 0.2204\ RI)\ (1.0 + 0.1359\ S_f) \quad ...(7)$$

(iii) Ductility of HFFC: The ductility of HFFC, as expressed by the strain at 85 percent of peak strength in the descending portion of the stress-strain curve is increased with the increase in the specific surface factor (S_f). The observed strain at 85 percent of the peak strength is expressed in terms of the observed strain (ε_{fu}) at ultimate strength. A plot between the ratio $(\varepsilon_{0.85fu}/\varepsilon_{fu})$ and the specific surface factor (S_f) is given in Fig. 7. The following relationship is obtained between the above ratio and the specific surface factor (S_f):

$$(\varepsilon_{0.85fu}/\varepsilon_{fu}) = (2.1127 \pm 0.064) + (0.0338 \pm 0.006)\ S_f \quad ...(8)$$

$$\varepsilon_{0.85fu} = \varepsilon_{fu}(2.1127 + 0.0338\ S_f) \quad ...(9)$$

In order to assess the contribution of ferrocement shell towards ductility improvement over Confined Fiber Reinforced Concrete (CFRC), the observed strain at 85 percent of the peak strength of HFFC is expressed in terms of the strain at 85 percent of the peak strength($\varepsilon_{0.85u}$) of corresponding confined fiber reinforced concrete (CFRC)(i.e., without any ferrocement shell confinement). A plot between the ratio $(\varepsilon_{0.85fu}/\varepsilon_{0.85u})$ and the specific surface factor (S_f) is given in Fig. 8, Which indicates the improvement of ductility with the specific surface factor over and above that of confined fiber reinforced concrete.. The following relationship is obtained between the ratio $(\varepsilon_{0.85fu}/\varepsilon_{0.85u})$ and the specific surface factor (S_f) :

$$(\varepsilon_{0.85fu}/\varepsilon_{0.85u}) = 1.163 + 0.2161S_f \quad ...(10)$$

Where,

$\varepsilon_{0.85u}$ = Strain at 85 percent of the peak strength of tie confined fiber reinforced concrete(CFRC)[14]

$$= \varepsilon_c'(1.9 + 9.88\ C_f)(0.842 + 0.276\ RI) \quad ...(11)$$

$$\varepsilon_{0.85fu} = \varepsilon_c'(1.9 + 9.88\ C_f)(0.842 + 0.276\ RI)(1.163 + 0.2161S_f) \quad ...(12)$$

Further the area under stress-strain curves, representing toughness, increased with the increasing specific surface factor (S_f) for a particular value of tie confinement level (C_f) and Reinforcing index (RI) of steel fiber. This gives an indication that for the same level of Energy absorption, the tie spacing may be increased and quantity of steel fiber may be decreased with the ferrocement casing. This is advantageous in situations where congestion of reinforcement poses difficulty in casting.

Table 2 Test Results of HFFC Prisms

S.NO.	Desig-nation	C_i	RI	S_f	f_c' (MPa)	ε_c' (10^{-05})	f_u (MPa)	ε_u (10^{-05})	f_u' (MPa)	ε_{fu} (10^{-05})	$\varepsilon_{0.85fu}$ (10^{-05})	$\frac{\varepsilon_{fu}}{\varepsilon_u}$	$\frac{\varepsilon_{0.85fu}}{\varepsilon_{fu}}$	P (KN)	K_f	$\frac{\varepsilon_{0.85fu}}{\varepsilon_{0.85u}}$
(1)	(2)	(3)	(4)	(5)	(6)	(7)	(8)	(9)	(10)	(11)	(12)	(13)	(14)	(15)	(16)	(17)
A - Series																
1	A0	0.35	0	0	23.06	160	27.49	451	27.50	450	790	0.997	1.755	618.75	0.968	1.079
2	A1	0.35	0	4.5	23.06	160	27.49	451	29.80	900	2350	1.995	2.611	670.50	1.052	3.209
3	A2	0.35	0	9.0	23.06	160	27.49	451	32.00	1000	2400	2.217	2.400	720.00	1.132	3.278
4	A3	0.35	0	13.5	23.06	160	27.49	451	34.30	1200	3300	2.660	2.750	771.75	1.215	4.507
5	A4	0.35	0	18.0	23.06	160	27.49	451	36.00	1530	4580	3.390	2.990	810.00	1.277	6.255
B - Series																
6	B0	0.39	1.48	0	20.1	165	28.11	657	29.53	630	1260	0.958	2.0	664.43	0.999	1.062
7	B1	0.39	1.48	4.5	20.1	165	28.11	657	30.23	1000	2450	1.522	2.45	680.17	1.024	2.063
8	B2	0.39	1.48	9.0	20.1	165	28.11	657	32.63	1490	3540	2.267	2.38	734.18	1.108	2.982
9	B3	0.39	1.48	13.5	20.1	165	28.11	657	37.13	1600	3900	2.440	2.44	835.42	1.264	3.285
10	B4	0.39	1.48	18.0	20.1	165	28.11	657	39.53	2700	5790	4.10	2.14	889.43	1.348	4.877
C - Series																
11	C0	0.37	2.95	0	21.74	162	34.66	776	33.6	760	1520	0.979	2.0	756	0.944	1.019
12	C1	0.37	2.95	4.5	21.74	162	34.66	776	36.5	930	2220	1.198	2.38	821.25	1.028	1.489
13	C2	0.37	2.95	9.0	21.74	162	34.66	776	37.5	1200	3120	1.546	2.60	843.75	1.056	2.093
14	C3	0.37	2.95	13.5	21.74	162	34.66	776	39.5	2000	5100	2.577	2.55	888.75	1.114	3.421
15	C4	0.37	2.95	18.0	21.74	162	34.66	776	42.0	2250	6000	2.899	2.66	945	1.186	4.025
D - Series																
16	D0	0.41	0	0	23.54	180	28.84	563.76	29.6	570	1050	1.011	1.842	666	0.996	1.164
17	D1	0.41	0	3.2	23.54	180	28.84	563.76	31.2	750	1600	1.33	2.133	702	1.052	1.774
18	D2	0.41	0	6.4	23.54	180	28.84	563.76	32.4	1020	2220	1.809	2.176	729	1.093	2.461
19	D3	0.41	0	9.6	23.54	180	28.84	563.76	34.5	1200	3150	2.128	2.625	776.25	1.166	3.492
20	D4	0.41	0	12.8	23.54	180	28.84	563.76	36.9	1700	4080	3.01	2.40	830.25	1.249	4.523
E - Series																
21	E0	0.4	0.74	0	22.9	200	30.69	710	33.0	690	1380	0.971	2.0	742.5	1.046	1.126
22	E1	0.4	0.74	3.2	22.9	200	30.69	710	34.3	1000	2200	1.408	2.2	771.75	1.089	1.796
23	E2	0.4	0.74	6.4	22.9	200	30.69	710	35.9	1330	3120	1.873	2.346	807.75	1.141	2.548
24	E3	0.4	0.74	9.6	22.9	200	30.69	710	38.0	1770	4290	2.492	2.423	855	1.209	3.503
25	E4	0.4	0.74	12.8	22.9	200	30.69	710	40.0	2200	4920	3.09	2.236	900	1.275	4.018

Table 2 Test Results of HFFC Prisms (cont.)

S.NO.	Desig-nation	C_i	RI	S_f	f_c' (MPa)	ε_c' (10^{-05})	f_u (MPa)	ε_u (10^{-05})	f_u' (MPa)	ε_{fu} (10^{-05})	$\varepsilon_{0.85fu}$ (10^{-05})	$\frac{\varepsilon_{fu}}{\varepsilon_u}$	$\frac{\varepsilon_{0.85fu}}{\varepsilon_{fu}}$	P (KN)	K_f	$\frac{\varepsilon_{0.85fu}}{\varepsilon_{0.85u}}$
(1)	(2)	(3)	(4)	(5)	(6)	(7)	(8)	(9)	(10)	(11)	(12)	(13)	(14)	(15)	(16)	(17)
F - Series																
26	F0	0.4	2.21	0	23	195	35.05	887	36.3	840	1800	0.947	2.143	816.75	1.01	1.068
27	F1	0.4	2.21	3.2	23	195	35.05	887	38.4	1200	2660	1.353	2.216	864	1.07	1.578
28	F2	0.4	2.21	6.4	23	195	35.05	887	40.60	1590	3890	1.792	2.446	913.5	1.133	2.308
29	F3	0.4	2.21	9.6	23	195	35.05	887	42.60	2060	5150	2.32	2.5	958.5	1.19	3.056
30	F4	0.4	2.21	12.8	23	195	35.05	887	43.80	2600	6890	2.931	2.65	985.5	1.225	4.089
G - Series																
31	G0	0.37	0	0	26.25	190	31.59	555.6	31.8	520	1090	0.936	2.096	710.78	0.986	1.226
32	G2	0.37	0	3.79	26.25	190	31.59	555.6	33.0	850	1960	1.53	2.305	742.5	1.03	2.205
33	G3	0.37	0	5.68	26.25	190	31.59	555.6	34.10	1000	2460	1.799	2.46	767.25	1.065	2.767
34	G4	0.37	0	7.58	26.25	190	31.59	555.6	36.00	1200	2930	2.159	2.44	810	1.125	3.290
H - Series																
35	H0	0.37	0.98	0	26.25	210	35.49	740.87	35.60	720	1530	0.972	2.125	801	0.99	1.178
36	H2	0.37	0.98	3.79	26.25	210	35.49	740.87	36.8	1200	2760	1.619	2.30	828	1.025	2.126
37	H3	0.37	0.98	5.68	26.25	210	35.49	740.87	38.3	1440	3530	1.944	2.45	861.75	1.066	2.719
38	H4	0.37	0.98	7.58	26.25	210	35.49	740.87	40.3	1580	4000	2.133	2.53	906.75	1.123	3.081
I - Series																
39	I0	0.37	1.97	0	26.25	205	38.66	852.96	38.60	840	1800	0.984	2.14	868.50	0.987	1.140
40	I2	0.37	1.97	3.79	26.25	205	38.66	852.96	40.40	1440	3230	1.688	2.24	909.00	1.033	2.046
41	I3	0.37	1.97	5.68	26.25	205	38.66	852.96	42.20	1730	4150	2.028	2.398	949.5	1.08	2.629
42	I4	0.37	1.97	7.58	26.25	205	38.66	852.96	43.70	1860	4530	2.180	2.43	983.25	1.118	2.870
J - Series																
43	J0	0.4	2.95	0	24.25	210	39.11	1060.8	38.7	1040	2130	0.98	2.04	870.75	0.989	1.046
44	J2	0.4	2.95	3.79	24.25	210	39.11	1060.8	40.60	1690	3790	1.59	2.24	913.50	1.038	1.862
45	J3	0.4	2.95	5.68	24.25	210	39.11	1060.8	42.80	1990	4540	1.875	2.28	963.0	1.095	2.230
46	J4	0.4	2.95	7.58	24.25	210	39.11	1060.8	44.0	2200	5260	2.074	2.39	990.00	1.126	2.584

$$K_f = \left[\frac{P - A_s f_y}{f_u A_g}\right] = \text{Load ratio}$$

$f_u = f_c'(1.0 + 0.55\ C_i)\ (1.0228 + 0.1024\ RI)$ = Strength of Tie Confined Fiber Reinforced concrete (CFRC)[14]

$\varepsilon_u = \varepsilon_c'(1.0 + 5.2\ C_i)\ (0.9899 + 0.2204\ RI)$ = Strain at peak of Tie Confined Fiber Reinforced Concrete (CFRC)[14]

$\varepsilon_{0.85u} = \varepsilon_c'(1.9 + 9.88\ C_i)\ (0.842 + 0.276\ RI)$ = Strain at 85 % of peak strength in the descending portion of stress - strain curve of CFRC[14]

f_u' = Strength of Hybrid Ferro Fiber Concrete prism

ε_{fu} = Strain at peak of Hybrid Ferro Fiber Concrete

$\varepsilon_{0.85fu}$ = Strain at 85 % of peak strength in the descending portion of stress - strain curve of HFFC

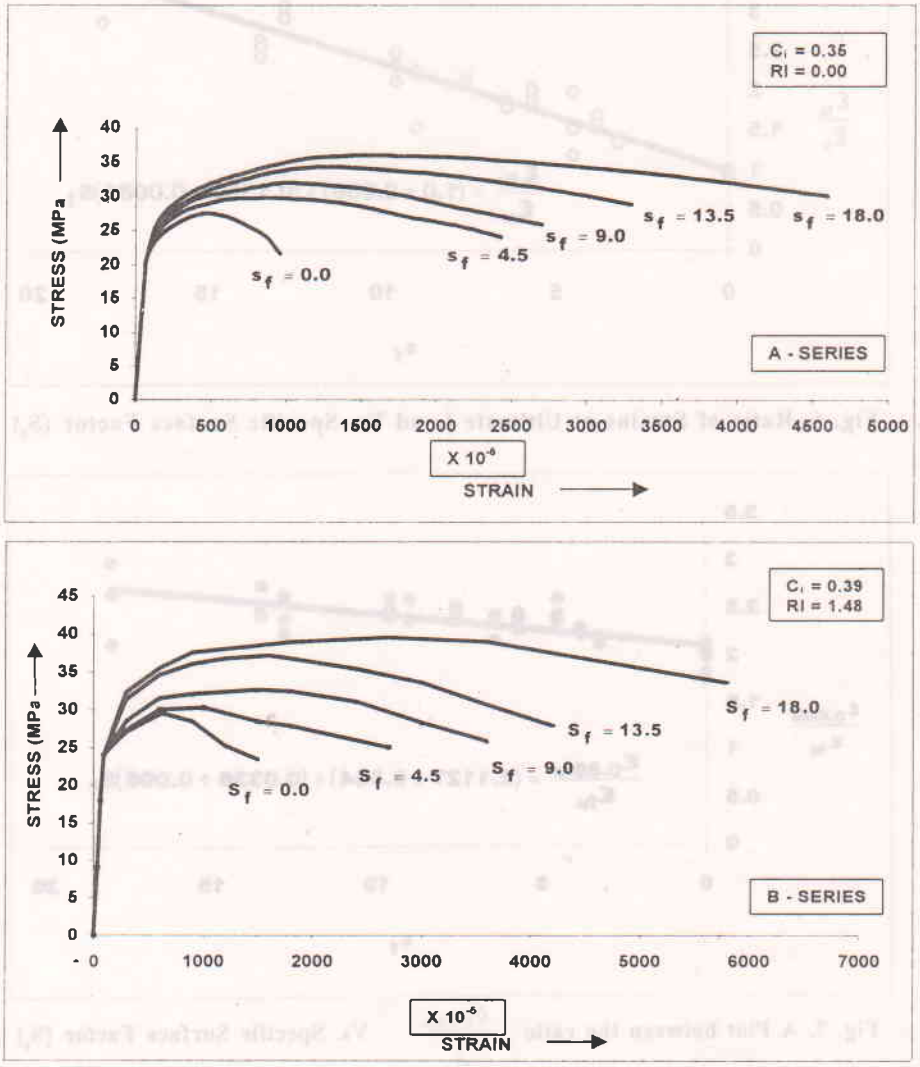

Fig. 4. Experimental Stress-Strain Curves of HFFC Prisms

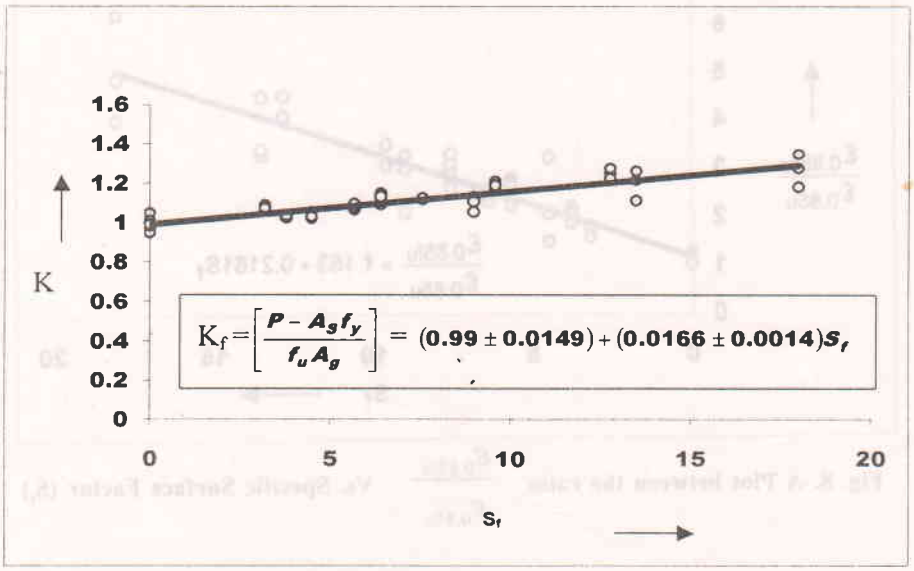

Fig. 5. Load Ratio (K_f) Vs. Specific Surface Factor (S_f)

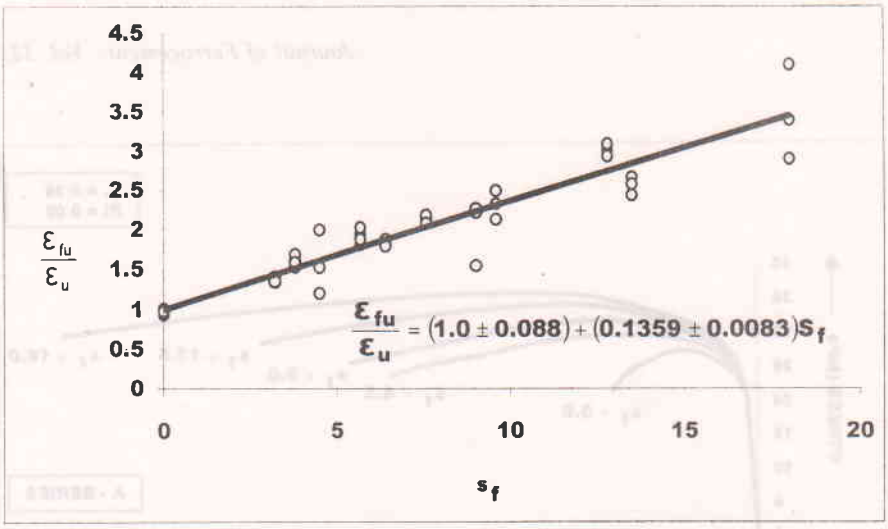

Fig. 6. Ratio of Strains at Ultimate Load Vs. Specific Surface Factor (S_f)

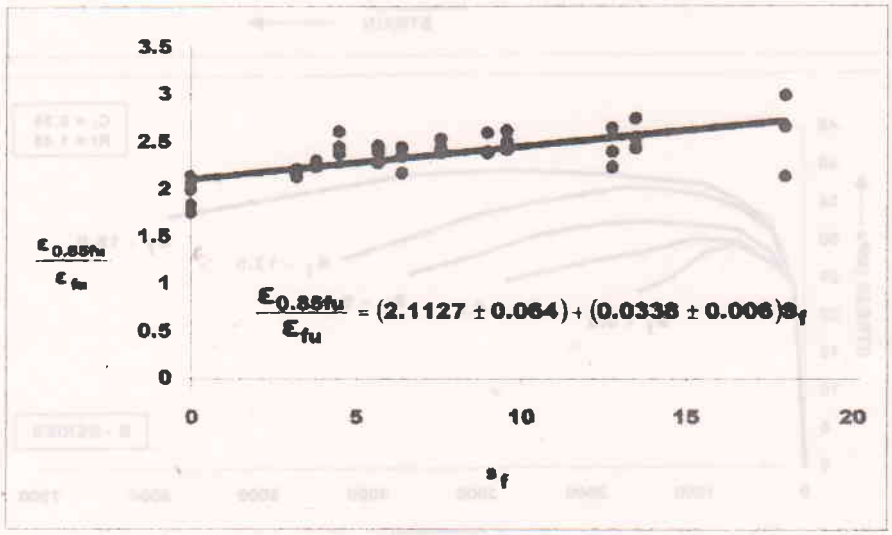

Fig. 7. A Plot between the ratio $\frac{\varepsilon_{0.85fu}}{\varepsilon_{fu}}$ Vs. Specific Surface Factor (S_f)

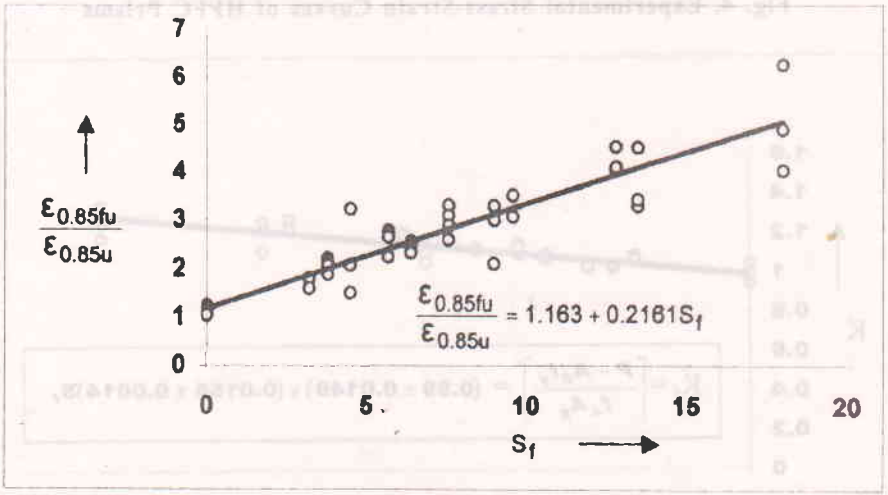

Fig. 8. A Plot between the ratio $\frac{\varepsilon_{0.85fu}}{\varepsilon_{0.85u}}$ Vs. Specific Surface Factor (S_f)

CONCLUSIONS

The following conclusions can be drawn from the experimental investigation on HFFC.

1. A ferrocement shell is an effective way of providing additional confinement to fiber reinforced concrete in axial compression and has the advantage over lateral tie confinement of improving material performance under large deformations.
2. The additional confinement with ferrocement shell improved the ultimate strength, strain at peak strength and ductility of fiber reinforced concrete.
3. The improved peak strength with ferrocement shell confinement varied linearly with the specific surface factor (S_f), and can be expressed by a linear relationship, which includes three parameters C_i, RI and S_f. The predicted equation for peak load carrying capacity of an HFFC prism is

$$P = f_c' (1 + 0.55C_f) (1.0228 + 0.1024\, RI) (1.0 + 0.0166\, S_f) A_g + f_y A_s$$

4. The improved strain at ultimate strength of HFFC prism can be expressed as

$$\varepsilon_{fu} = \varepsilon_c' (1.0 + 5.2\, C_f) (0.9899 + 0.2204\, RI) (1.0 + 0.1359\, S_f)$$

5. The ductility of HFFC, as expressed by the strain at 85 percent of peak strength in the descending portion of stress-strain curve is increased with the increase in the specific surface factor (S_f) and can be expressed as:

$$\varepsilon_{0.85fu} = \varepsilon_c' (1.9 + 9.88\, C_f)(0.842 + 0.276\, RI)(1.163 + 0.2161 S_f)$$

6. For higher levels of confinement in fiber reinforced concrete, there exists equivalent lower level confinement in Hybrid ferro fiber concrete (HFFC). Hence, some amount of confining transverse reinforcement and quantity of steel fiber can be replaced by providing ferrocement shell as casing to the fiber reinforced concrete. This will ease the situation like seismic resistant beam column junctions where high confinement requirement leads to congestion of steel.

REFERENCES

1. Alsayed, S.H.1992, Confinement of Reinforced Concrete Columns by Rectangular Ties and Steel Fibers. *Magazine of Concrete Research*, 44(161): 265-270.
2. Ahmad, S.H.; and Shah, S.P.1982, Stress-strain curves of Concrete Confined by Spiral Reinforcement. *ACI Journal Proceedings*, 79(6): 484-490.
3. Blume, J.A., et al., 1961, Design of multistory reinforced concrete buildings for earthquake motions. Portland Cement association, USA.
4. Ganesan, N; and Anil, J. 1993. Strength and behavior of RC columns confined by ferrocement. *Journal of Ferrocement*, 23(2): 99-108.
5. Ganesan, N; Ramanamurthy, J.V.1990. Strength and behavior of confined steel fiber reinforced concrete columns. *ACI Materials Journal*, 87(3): 221-227.
6. IS 456 – 2000. *Indian Standard Code of Practice for Plain and Reinforced Concrete*. Delhi: Indian Standards.

7. IS 8112 – 1981. *Specifications for 43 Grade Ordinary Portland Cement*. Delhi: Indian Standards.
8. Pama, R.P.; Robles-Austriaco, L.R.; and Rubio-Hermosura, N. 1993. Current researches on ferrocement. *Journal of Ferrocement*, 23(4): 227-288.
9. Paulay and Priestley, M.J.N. 1992. *Seismic Design of Reinforced Concrete Concrete and Masonry Buildings*. New York: John Wiley and Sons.
10. Reddy, S.R. 1974. Behavior of Concrete Confined in Rectangular Binders and its Applications in Flexure of Reinforced Concrete Structures, Ph.D. Thesis, J.T.University, Hyderabad, India.
11. Rao, C.B.K. and Rao, A.K. 1986. Stress strain curve in axial compression and Poisson's ratio of ferrocement. *Journal of Ferrocement*, 16(2): 117-128.
12. Rao, A.K.; Reddy, K.N.; and Reddy, V.M. 1979. Effect of stirrup confinement on flexural behavior of prestressed concrete beams. *Journal of IE(India)* 59: 258-266.
13. Ramesh, K.; Seshu, D.R.; and Prabhakar, M. 2000. Confined fiber reinforced concrete (CFRC). *Proceedings of Twenty Fifth Anniversary International Conference on Our World in Concrete and Structures*, 531-537. Singapore: CI – Premier Pvt. Ltd.
14. Ramesh, K.; Seshu, D.R.; and Prabhakar, M. 2000. A study of tie confined fiber reinforced concrete under axial compression. *RILEM Journal of Concrete Science and Engineering*, 02: 230-236.
15. Seshu, D.R., and Rao, A.K. 1998. Behavior of ferrocement confined reinforced concrete(FCRC) under axial compression. *RILEM Materials and Structures Journal*, 31: 628-633.
16. Waliuddin, A.M., et al. 1994. Study of behavior of plain concrete confined with ferrocement. *Journal of Ferrocement*, 24(2): 139-145.